

Received May 8, 2020, accepted June 12, 2020, date of publication June 16, 2020, date of current version June 30, 2020.

Digital Object Identifier 10.1109/ACCESS.2020.3002883

# Multi-Purpose Oriented Real-World Underwater Image Enhancement

ZETIAN MI<sup>1</sup>, YUANYUAN LI<sup>1</sup>, YAFEI WANG<sup>1</sup>, AND XIANPING FU<sup>1,2</sup>

<sup>1</sup>College of Information Science and Technology, Dalian Maritime University, Dalian 116026, China

<sup>2</sup>Peng Cheng Laboratory, Shenzhen 518055, China

Corresponding author: Yafei Wang (wangyafei@dmlu.edu.cn)

This work was supported in part by the National Natural Science Foundation of China under Grant 61802043, in part by the Liaoning Revitalization Talents Program under Grant XLYC1908007, in part by the Foundation of Liaoning Key Research and Development Program under Grant 201801728, in part by the Fundamental Research Funds for the Central Universities under Grant 3132020215 and Grant 3132016352, and in part by the Dalian Science and Technology Innovation Fund under Grant 2018J12GX037 and Grant 2019J11CY001.


**ABSTRACT** Images captured underwater usually suffer from weak illumination, color cast, fuzz and noise, which severely degrade the visibility. Numerous methods have been proposed to improve the quality of underwater images, but rarely of them can give a comprehensive consideration to all these problems, which makes them hard to adapt for various and complex real-world underwater scenes. Herein, a novel multi-purpose oriented approach for real-world underwater image enhancement is proposed. To manipulate different information on the corresponding layers, we firstly decompose the input image into illumination layer and reflectance layer. Subsequently, compensation of the brightness is carried out on the illumination layer, while color correction and contrast enhancement are implemented on the reflectance layer through a multi-scale processing strategy. Benefiting from this strategy, the proposed approach is provided with high control flexibility, which can significantly improve the visibility of underwater images while efficiently suppress the amplification of noise. Both qualitative and quantitative evaluations demonstrate that the proposed method has superior robustness, accuracy and effectiveness for complex marine circumstance.

**INDEX TERMS** Real-world underwater image enhancement, multi-purpose oriented, various water types, gradient domain.

## I. INTRODUCTION

Due to the shortage of resources on land, undersea world has obtained considerable attention. Acquisition of clear underwater images and videos play a pivotal role in a wide range of ocean applications. However, since the light received by a camera suffers from strong wavelength-dependent absorption and scattering, images and videos acquired under water are typically degraded with weak illumination, color distortion and low contrast. What's more, large amounts of suspended particles and marine snow introduce obvious noise. These unfavorable visibility further decreases the accuracy rate of underwater object detection and pattern recognition. Thus, developing an effective method to restore such images is desirable.

To solve the problems mentioned above, a variety of underwater image enhancement and restoration methods have

The associate editor coordinating the review of this manuscript and approving it for publication was Orazio Gambino .

been proposed. Earlier methods mainly rely on hardware processing, such as range-gated laser imaging system [1] or polarization filters [2], which are limited in practical applications. Recently, the vast majority of methods focus on utilizing the information from a single image to improve the visual quality. In order to correct the color cast and enhance the visibility, many image enhancing techniques, such as white balance, color correction, histogram equalization, fusion-based methods [3] and Retinex-based methods [4]–[6], are developed. Without considering the physical imaging process, this kind of method is less applicable for underwater scenario with complex physical properties. What's more, noise that is less obvious in the raw underwater image will be significantly amplified.

Inspired by the similarity between the distortion process of outdoor hazy and underwater scenes, attempts have been made using the image formation model (IFM), in which the transmission is usually estimated by the well known Dark Channel Prior (DCP) [7]. However, since the attenuation of

light under water is wavelength-dependent and less homogeneous than in outdoor, DCP-based methods show severe limitations. Although physical characteristics of water are incorporated in the improved DCP [8]–[10], it still hard to adapt for various water types.

With the remarkable success achieved by deep-learning in computer vision, more and more deep models are proposed. But in fact, the performance of these methods remains unsatisfactory due to the lack of dataset, which contains both the real-world underwater images and their corresponding ground truths for different water types. Although several strategies are introduced to simulate underwater image, there still exists a gap between synthetic and real-world underwater images [11].

Even though great progress on underwater restoration has been made, the existing algorithms focus solely on compensating either light scattering or color distortion, rarely of them concern about the low-light and noisy circumstance, which are ubiquitous during deep-sea exploration. To address the aforementioned problems, a novel multi-purpose oriented framework is proposed for real-world underwater image enhancement, which aims at handling diverse images captured under complex marine circumstances. First, we separate the input image into illumination and reflectance. The estimated illumination represents the luminance, while the reflectance illustrates the actual contrast and color. Subsequently, according to the visual quality of the input image, a pair of improved illumination and reflectance is produced using different post-processing strategies. In this way, the brightness, contrast and color can be restored simultaneously. Meanwhile, noise caused by suspended particles and marine snow is also significantly suppressed. Since guided by the actual optical process, the proposed method is suitable for different water types and shown superior robustness, accuracy and flexibility. The specific contributions are summarized as follows:

- To deal with the limitations faced by existing underwater image restoration methods in complex real-world scenes, a multi-purpose oriented approach is proposed. It can comprehensively address the challenging problems of real-world underwater images. By capturing different information into the corresponding layers, the proposed approach can effectively compensate brightness, color and contrast simultaneously without the significant amplification of noise.
- Rather than relying on specific assumptions or priors to accurately estimate parameters derived from IFM, the proposed approach only uses the optical properties to measure the attenuation rate of the input image, thereby indicating the amplitude of compensation. Without solving the IFM, the proposed method takes advantages of both enhancement-based and physical-model-based categories, which can adapt to various water types.
- Due to suspended particles and weak illuminance in real underwater world, the captured images and videos suffer from large amount of noise. Existing methods

tend to enhance noise substantially when restoring the contrast. Motivated by our previous work in dealing with outdoor hazy scenes, the proposed method captures different level of details into the corresponding layers. By controlling the enhancement amplitude of different layers, we can generate visually appealing results while limit the amplification of noise.

The rest of the paper is organized as follows. In Section II, numerous related works are reviewed. The proposed method is detailed in Section III. Section IV reports the qualitative and quantitative experimental results. Section V summarizes the conclusion.

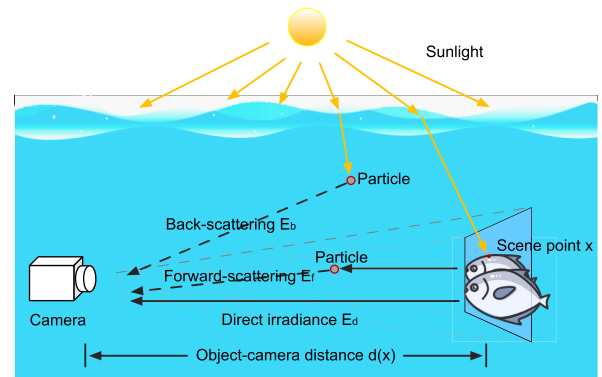


FIGURE 1. Underwater imaging model [12].

II. RELATED WORK

A. UNDERWATER IMAGING MODEL

According to the underwater imaging model proposed by McGlamery [13], as shown in Figure.1, it is believed that the total optical radiation received by the underwater imaging system consists of three parts: (1) the direct component  $E_d$ , that is the light reflected by the object without scattering; (2) the forward-scattering component  $E_f$ , that is the light scattering away from the propagation trajectory and finally reaching the imaging device; (3) the back-scattering component  $E_b$ , which is the ambient light scattered by suspended particles. The total optical radiation  $E_T$  can be represented as the linear superposition of the above three components and shown as follows:

$$E_T(x, y) = E_d(x, y) + E_f(x, y) + E_b(x, y) \tag{1}$$

where  $(x, y)$  is the coordinate of the pixel. Since the distance between the camera and the underwater scene is relatively close, the forward-scattering component can be ignored [8], [14].

If we define  $J(x, y)$  as the scene radiance,  $t(x, y)$  as the transmission (decreasing exponentially with the depth of the scene) and  $B$  as the background light. Then the scene  $I(x, y)$  captured by the camera can be represented as:

$$\begin{aligned} I^c(x, y) &= E_d(x, y) + E_b(x, y) \\ &= J^c(x, y)t^c(x, y) + B^c(1 - t^c(x, y)) \end{aligned} \tag{2}$$

$c \in \{r, g, b\}$

Generally, Eq.2 is considered as the simplified underwater imaging model (IFM), which is similar with the optical imaging model in the atmosphere. Therefore, outdoor image restoration technologies are gradually applied into the underwater scenes.

In addition, the attenuation of light under water is wavelength-dependent [8], [14]. When traveling through water, the red light having a longer wavelength is absorbed faster than blue and green light, which leads to the blue-green tone of underwater images. It worth mentioning that the strong attenuation of one color channel can dramatically affect the performance of most existing outdoor restoration techniques [15].

Numerous approaches have been proposed to improve the visual quality of underwater image. With different core concept, they can be lumped into three categories.

### B. UNDERWATER IMAGE ENHANCEMENT METHOD

In this line of research, methods aim at correcting the color cast and enhancing the contrast by manipulating image pixels. Iqbal *et al.* [16] stretch the histogram in RGB color space and balance the saturation in HSV color space. Fu *et al.* [17] proposes a two-step enhancement method, which carries out a color correction process followed by a contrast enhancement process. In order to utilize the complementary information of multiple images to generate high-quality result, Ancuti *et al.* [3] employ a multi-scale fusion method by fusing a contrast enhanced image and a color corrected image derived from the single input image. Most recently, to improve image enhancement in terms of color appearance, Ancuti *et al.* [15] introduce a fundamental color channel compensation (3C) pre-processing step for image enhancement. They observe that information contains in at least on color channel of images with non-uniform color spectrum distribution is close to completely lost. By reconstructing the lost channel based on the opponent color channel, the 3C algorithm consistently improves the outcome of conventional restoration methods.

With the same goal of our proposed method, Retinex-based methods have been proposed. Zhang *et al.* [4] apply multi-scale retinex into underwater image enhancement. Fu *et al.* [5] firstly correct the color cast, and then enhance the contrast using retinex-based model. In order to adapt to both low illumination image and underwater image, Dai *et al.* [6] employs different strategies on the incident light and then improves the contrast of the reflectance.

These enhancing-based methods do not consider the physical properties of underwater imaging mechanism, so that the results tend to bring out artifacts, over-enhancement or color distortion. Meanwhile, noise caused by suspended particles and marine snow will be significantly amplified.

### C. UNDERWATER IMAGE RESTORATION METHOD

Due to the high similarity between the optical imaging process of underwater and outdoor hazy scenes. The simplified image formation model (IFM) as shown in Eq.2 has

been introduced to describe the underwater scene. To estimate the derived parameters, the well known Dark Channel Prior (DCP) [7] is used. However, owing to the wavelength-dependent absorption and inhomogeneous medium under water, traditional DCP shows significant limitations, leading to erroneous transmission estimation and poor restoration results. Therefore, physical properties of water are embedded into the modified DCP. In [8], Chiang *et al.* combine wavelength compensation with a classic dehazing algorithm to restore underwater image. Galdran *et al.* [18] propose a red channel prior, whose DCP is carried on green, blue and the inverted red channels. While in [19]–[21], DCP is applied on only the green and blue channels. Since the information of red channel is not dependable in diverse underwater scenes based on the analysis of UDCP [9], the maximum intensity prior (MIP) [22] and blurriness-based [23] approaches are proposed. To dealing with the low-light deep-sea circumstance, Li *et al.* [24] proposes an adaptive bright-color channel based low-light underwater enhancement method followed by a denoising and a color correction method to enhance such images and remove noise and artifacts. In [10], Yang *et al.* combine maximum scene depth estimation and adaptive color correction to accurately estimate the background light. To taking advantage of both the image-based and model-based approaches, Chang [25] compute two transmission maps from distinct perspectives and fuse them weighted by their saliency maps. Also, two different approaches are used to integrate the background light into a more accurate estimation. The final outcome is dissolved through a point spread function deconvolution and color compensation. Based on the assumption that the depth of patches changes gradually in a local neighborhood for outdoor scenes, Mandal and Rajagopalan [26] introduces a local proximity method for hazy image enhancement. By considering the effect of atmospheric model parameters, local haziness is reformulated and parameters are estimated locally depending on the haze condition. Without relying on any empirical assumption of airlight, they also adopt the local proximity method into underwater image restoration but obtain obvious over-saturated results.

With regards to the optical properties under water, the model-based methods aim at estimating the transmission map (or depth map) and background light as accurate as possible to solve the IFM model for image restoration. However, even if the transmission or background light is relatively well estimated by these methods, undesired color shifts or visually displeasing results are still inevitable. This is because that specific assumptions and priors may not always hold in the diverse and complex marine circumstance.

### D. DEEP-LEARNING BASED METHOD

This kind of method concentrate on learning the mapping function between synthetic underwater images and their corresponding ground truths. Nevertheless, it is practically impossible to obtain the ground truth for image captured under different water types. Benefit from the Generative

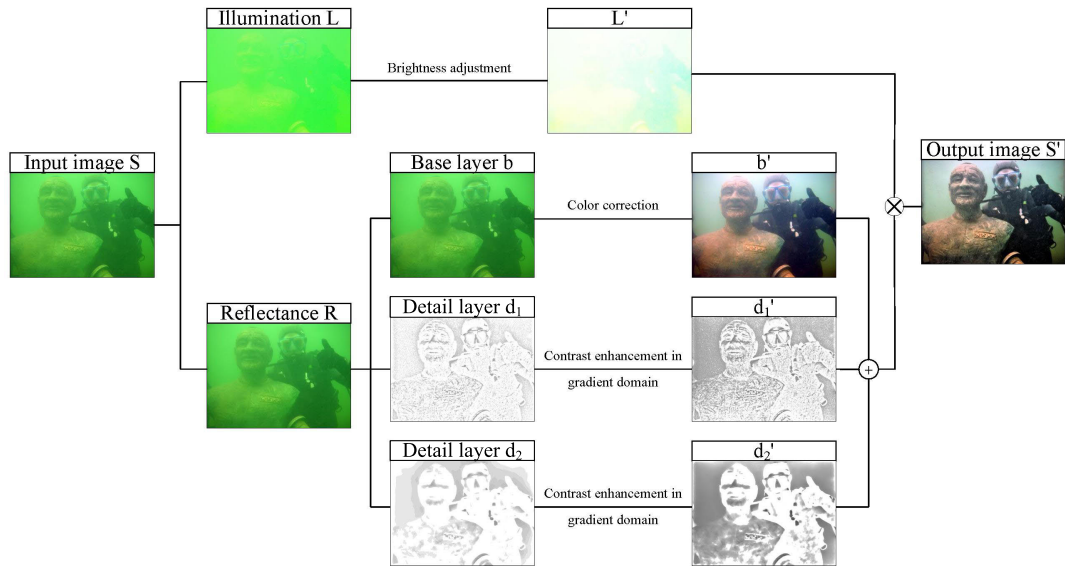


FIGURE 2. Flowchart of the proposed method. (Detail layers are reversed in order to facilitate the display).

Adversarial Networks, Li *et al.* [27] proposes a WaterGAN, which synthesis underwater images using inair clear image and depth pairs to train the restoration network. Most recently, an increasing number of deep-learning based methods are introduced, e.g. UWCNNs [28], UGAN [29], Water CycleGAN [30], DenseGAN [31] *et al.* These methods all try hard to get rid of the limitation of dataset and broaden the applicability of the algorithm. However, lacking sufficient training data and uncertain outputs tend to make the performance of deep-learning based methods largely unsatisfactory, and whose robustness and generalization still fall behind the conventional state-of-the-art methods. To solve the difficulty in the deep-learning based underwater image enhancement, Li *et al.* [11] construct a large scale real-world underwater image enhancement benchmark dataset (UIEBD), which contains totally 950 real-world underwater images for further research.

### III. THE PROPOSED METHOD

In this section, a multi-purpose oriented approach is proposed to enhance real-world underwater images, which can restore the brightness, color and contrast simultaneously. The proposed method contains three main steps: estimation of the illumination and the reflectance, multi-scale decomposition of the reflectance, and post-processing on different image layers for restoration of weak illuminance, color cast and fuzz. The flowchart of the framework is shown in Figure.2.

#### A. ESTIMATION OF THE ILLUMINATION AND THE REFLECTANCE

Since underwater images are generally captured under low-light conditions, Retinex model is uniformly applied in this case. According to the Retinex theory, a captured image can

be described as:

$$S^c(x, y) = R^c(x, y) \cdot L^c(x, y), \quad c \in \{r, g, b\} \quad (3)$$

where  $S$  is the captured image,  $R$  is the reflectance and  $L$  is the illumination.  $(x, y)$  is the coordinate of the pixel.  $c$  represents the color channel in RGB color space.

In order to improve the brightness and the contrast jointly, we separate the illumination, which is piece-wise smooth and contains the illuminance variance, from the reflectance using the Retinex theory. In this way, the global incident light of the scenario is captured in the illumination, while color information and details are preserved in the reflectance. Subsequently, different post-processing strategies are applied on the corresponding image layers to compensate the illuminance, color and contrast separately.

To effectively estimate illumination and reflectance from the single input image, most variational methods use the logarithmic transformation for pre-processing to simplify the ill-posed problem. However, the variation of gradient magnitude is typically suppressed in the logarithmic domain, which leads to over-smoothed reflectance with much of the desired edges and texture details lost. To this end, the weighted variational model proposed by Fu *et al.* [32] is utilized to estimate the illumination and the reflectance simultaneously. The objective function is:

$$\begin{aligned} \arg \min_{r, l} & \|r + l - s\|_2^2 + c_1 \|e^r \cdot \nabla r\|_1 + c_2 \|e^l \cdot \nabla l\|_2^2 \\ \text{s.t. } & r \leq 0 \quad \text{and} \quad s \leq l \end{aligned} \quad (4)$$

where  $s = \log(S)$ ,  $r = \log(R)$  and  $l = \log(L)$ ,  $c_1$  and  $c_2$  are two positive parameters.  $\nabla$  is the gradient variation and  $\|\cdot\|_p$  denotes the p-norm operator. The first term  $\|r + l - s\|_2^2$  is used to maintain the fidelity, minimizing the distance between  $(r + l)$  and  $s$ . The second term  $\|e^r \cdot \nabla r\|_1$  enforces piece-wise

constant on  $r$ . And the third term  $\|e^l \cdot \nabla l\|_2^2$  enforces spatial smoothness on  $l$ .

To simplify the minimization of the objective function (2), and eliminate the impact of the weights  $e^r$  and  $e^l$ , the objective function can be rewritten as:

$$\begin{aligned} \arg \min_{r^k, l^k} &= \|r^k + l^k - s\|_2^2 + c_1 \|R^{k-1} \cdot \nabla r^k\|_1 \\ &+ c_2 \|L^{k-1} \cdot \nabla l^k\|_2^2 \\ \text{s.t. } &r^k \leq 0 \text{ and } s \leq l^k \end{aligned} \quad (5)$$

$k$  represents the  $k$ -th iteration. Subsequently, an alternating direction method of multipliers (ADMM) [33] is adopted to solve the new objective function. Figure.3 shows the estimated illumination and reflectance.

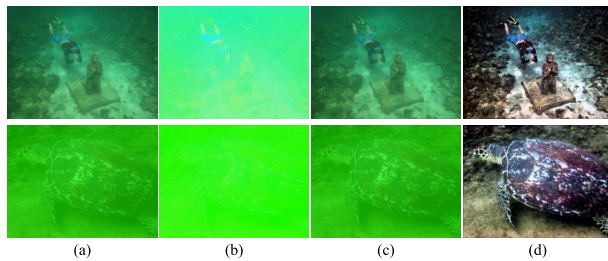


**FIGURE 3.** The estimated illumination and reflectance. (a) Raw underwater images. (b) The estimated illuminations. (c) The estimated reflectances. (d) Results of the proposed method.

### B. MULTI-SCALE DECOMPOSITION OF THE REFLECTANCE

Since conventional IFM-based methods strictly rely on the accuracy of the estimation of derived parameters, even if well estimated, the restored radiance after solving the optical model may still present undesired color artifacts. Although physical characteristics of water have been taken into consideration, specific suppositions and priors are still limited in diverse and complex water scenes. Herein, the ambition of this paper is in an attempt to develop a new framework for the restoration of complex real-world underwater images. To take advantage of both enhancement-based and model-based categories, a multi-scale gradient domain contrast enhancement approach is extended into underwater image restoration. Rather than estimating transmission or background light using modified DCP and solving the IFM, the proposed method only regards the fast estimated transmission as an indicator of the quality of the observed image, further providing guidance for the setting of enhancement coefficients. In this way, the proposed method can properly restore the underwater images that make exceptions to the conventional methods.

Firstly, to decompose the reflectance into multiple scales, weighted least squares (WLS) based filter [34] is considered to split the reflectance into a progressively smoother image sequence, which can be obtained by:

$$u = F_\lambda(R) = (I + \lambda L_R)^{-1} R \quad (6)$$

where  $u$  is the smoothed version of the reflectance  $R$ .  $I$  is the identity matrix.  $L_R = D_x^T A_x D_x + D_y^T A_y D_y$ , in which  $(x, y)$  is the spatial location of a pixel,  $D_x$  and  $D_y$  are discrete differentiation operation,  $A_x$  and  $A_y$  contain the smoothness weights. By increasing the positive parameter  $\lambda$ , the progressively smoother image sequence  $u^1, \dots, u^{k-1}$  can be produced.

Secondly, by subtracting subsequent coarser images, the multi-scale representation can be generated. The coarsest image  $u^{k-1}$  is served as the base layer  $b$ , which consists the color variation of the reflectance, while the detail layers  $d_i$  are computed as:

$$d_i = u^{i-1} - u^i, \text{ where } i = 1, \dots, k-1 \text{ and } u^0 = R. \quad (7)$$

$k = 3$  is set in our experiments.

It is worth mentioning that a larger smooth parameter  $\lambda$  can produce a smoother  $u^1$ . By subtracting  $u^1$  from  $R$ , most of small scale textures including noise and marine snow can be captured in the detail layer  $d_1$ . Therefore, by limiting the enhancement degree of  $d_1$ , significant noise amplification which is inevitable in existing underwater restoration technologies can be prevented.

### C. POST PROCESSING

After capturing information of brightness, color and contrast into the corresponding layer, post-processing is adopted to restore low-light, color distortion and fuzz problems simultaneously. As shown in the flowchart (Figure.2), brightness adjustment is carried out on the illumination  $L$ . Color correction is applied on the base layer  $b$  of the reflectance, while contrast enhancement is applied in the gradient domain of detail layers  $d_i$  in order to avoid the generation of artifacts.

#### 1) BRIGHTNESS ADJUSTMENT

Since the incident light variance is contained in the illumination, the frequent low-light problem is addressed on this layer in order to improve the global brightness. The enhanced illumination  $L'$  is computed as:

$$L'(x, y) = \text{sigmoid}(\alpha L(x, y)) \quad (8)$$

where  $\text{sigmoid}(\cdot)$  is the sigmoid function. Parameter  $\alpha$  controls the degree of luminance adjustment. In this paper, according to the experimental performance,  $\alpha$  is set to:

$$\alpha = 10 + (1 - L_{mean})/L_{mean} \quad (9)$$

where  $L_{mean}$  is the mean value of the illumination, which indicates the under-exposure degree of the input underwater image. Thus, smaller value of  $L_{mean}$  guides a higher magnitude of enhancement. Two examples of the brightness adjustment are shown in Figure.4.

#### 2) COLOR CORRECTION

Due to the wavelength-dependent attenuation of light under water, most underwater images appear blue or green. After decomposing the reflectance into multiple scales, the low frequency color variance is contained in the coarsest version

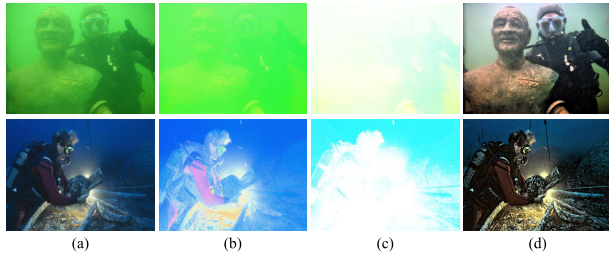


**FIGURE 4. Brightness adjustment. (a) Raw underwater images. (b) The estimated illuminations. (c) Illuminations after brightness adjustment. (d) Final results of the proposed method.**

of the reflectance, namely the base layer  $\mathbf{b}$ . Thus, color correction is realized in this layer to further restore the color distortion of the input underwater image. A Gaussian distribution based linear mapping model is adopted for color correction. Firstly, the maximum and minimum of  $\mathbf{b}$  in each channel is given by:

$$\begin{aligned} b_{max}^c &= b_{mean}^c + \mu b_{var}^c \\ b_{min}^c &= b_{mean}^c - \mu b_{var}^c \end{aligned} \quad (10)$$

where  $c \in \{r, g, b\}$ ,  $b_{mean}^c$  and  $b_{var}^c$  are the mean value and the standard deviation of the base layer  $\mathbf{b}$  in the  $c$  channel.  $\mu$  is a parameter controlling the image dynamic range and set to  $\mu = 2.3$  in our experiments. Finally, the color corrected base layer  $\mathbf{b}_{cr}^c$  is computed as:

$$\mathbf{b}_{cr}^c = \frac{\mathbf{b}^c - b_{min}^c}{b_{max}^c - b_{min}^c} \quad (11)$$

### 3) CONTRAST ENHANCEMENT

In order to significantly improve the structure and details of interest while avoid artifacts, the contrast of the underwater image is enhanced by manipulating the gradient domain of the reflectance, rather than solving the IFM. This strategy shows excellent textural details enhancement performance with efficient suppression of undesired artifacts and noise.

According to the IFM in Eq.2 [8], the contrast of the input image can be measured as:

$$\sum_x \|\nabla I(\mathbf{x})\| = t \sum_x \|\nabla J(\mathbf{x})\| \leq \sum_x \|\nabla J(\mathbf{x})\| \quad (12)$$

in which,  $\mathbf{x}$  is the coordinate of the pixel.  $I$  is the input image and  $J$  is the scene radiance. Transmission  $t$  conforms to  $t \leq 1$ .  $\nabla$  is the gradient operator. This equation indicates that the attenuation of  $\|\nabla J\|$  is associated with the transmission value. Since directly using the reciprocal of  $t$  as the enhancement coefficient, the denominator may close to zero causing severe artifacts, the average of  $t$  is applied instead of  $t$ . Therefore, contrast enhancement manipulated on the gradient domain of multi-scale detail layers of the reflectance is defined as:

$$\nabla d_i' = \frac{\omega_i}{\bar{t}} \nabla d_i \quad (13)$$

where  $\omega_i$  are non-negative parameters controlling the enhancement strength.  $\bar{t}$  is the average of  $t$ , in which  $t$

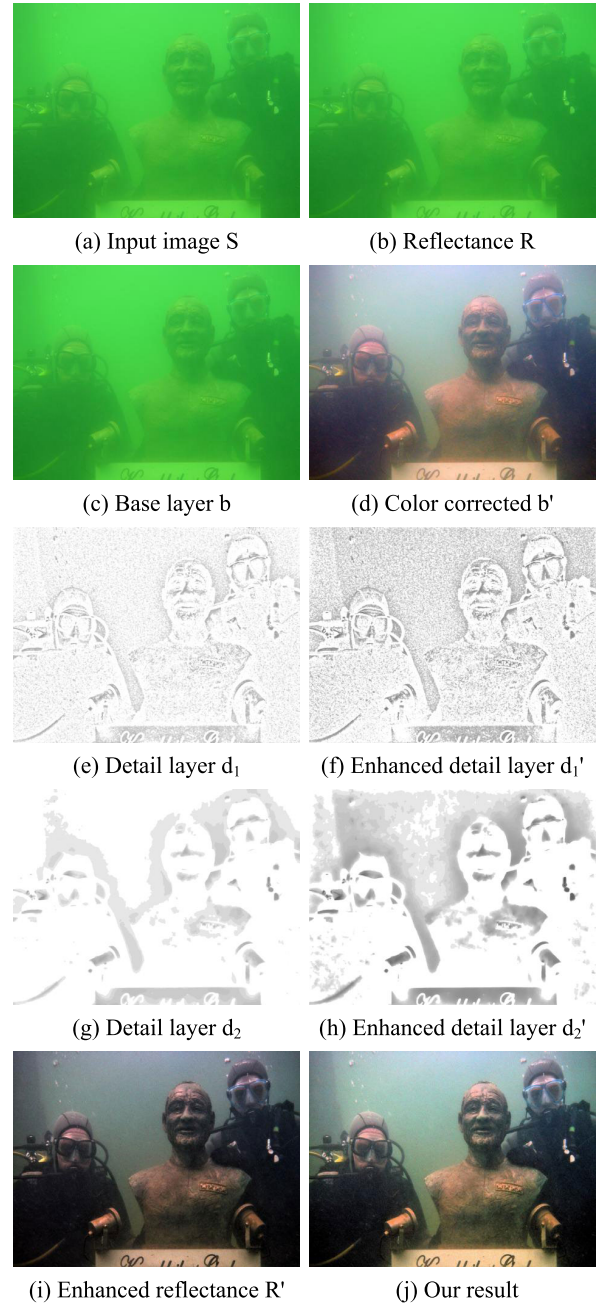


**FIGURE 5. Overview of the post-processing on the reflectance. (Detail layers are reversed to facilitate the display).**

is calculated by the fast method proposed by Tarel and Hautière [35]. As analyzed in Section III-B,  $d_1$  contains the most of tiny details including noise, which is desired to be enhanced slightly. While  $d_2$  captures significant structures and strong edges, it should be enhanced with a larger strength. That is,  $\omega_1 \leq \omega_2$  is set in most cases of our experiments. In this way, the proposed method is equipped with high control flexibility, which can simultaneously restore the visibility efficiently and suppress the significant amplification of noise. Figure.5 illustrates an overview of the post-processing on the reflectance.

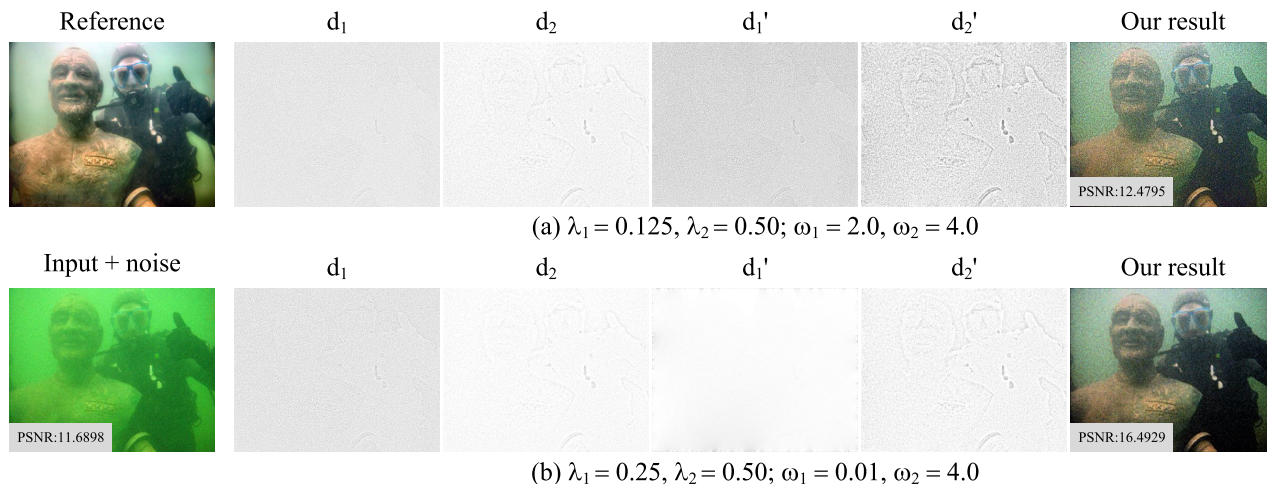


FIGURE 6. The performance of noise suppression with different parameter settings.

By solving a Poisson equation on the modified gradients, two enhanced detail layers  $d'_1$  and  $d'_2$  are obtained. Accordingly, the improved reflectance is given by:

$$R' = b_{cr} + d'_1 + d'_2 \tag{14}$$

and the restored result can be output by:

$$S' = R' \cdot L' \tag{15}$$

#### IV. EXPERIMENTAL RESULTS AND DISCUSSION

To evaluate the performance of the proposed method, comparisons are carried out against several state-of-the-art underwater image enhancement methods, including retinex-based [5], two-step [17], UDCP [9], UIBLA [23], GDCP [36], red channel [18] and fusion-based [3], both qualitatively and quantitatively. What's more, in order to further prove the adaptability of the proposed method in real-world complex underwater scenes, comparisons with several representative deep-learning based methods, i.e. WaterGAN [27], UGAN [29], UWCNN [28] and Water-Net [11], are also presented. The experiments are carried out on the Underwater Image Enhancement Benchmark (UIEB) [11] dataset, which includes 950 real-world underwater images in all. 890 of them have corresponding reference images which are considered to be the best restoration results selected by 50 volunteers, while the rest 60 underwater images cannot obtain satisfactory references and are treated as challenging data. In order to evaluate the performance of different methods fairly, source codes and the recommended parameter settings are applied in the experiments. For quantitative evaluation, full-reference criteria: peak signal to noise ratio (PSNR), patch-based contrast quality index (PCQI) [37], non-reference criteria: underwater image quality measure (UIQM) [38], underwater color image quality evaluation (UCIQE) [39] are used. For both the larger the metrics, the better the quality. Bold values represent the best results.

It takes about 15.9 seconds to process a color image with size of  $1024 \times 768$ . Three of the most time consuming steps: estimation of the illumination and the reflectance, multi-scale decomposition of the reflectance and manipulation of the gradient take about 20% (3.2 s), 33% (5.3 s) and 12% (1.9 s) of the whole running time, respectively.

#### A. ANALYSIS OF THE NOISE SUPPRESSION PERFORMANCE

In this section, the excellent effectiveness of the proposed method in suppressing the amplification of noise is presented and analyzed in detail. Generally, when generating the progressively smoother image sequence via Equation 6,  $\lambda_1 = 0.125, \lambda_2 = 0.50$  are set. Subsequently, by subtracting the subsequent coarser images we can obtain the multi-scale representation. As mentioned above, detail layer  $d_1$  contains most of the tiny details and noise, while  $d_2$  captures strong edges and significant structures. This mechanism brings up the high control flexibility of the proposed method. In order to present the big advantage, an experiment in extreme noisy condition is carried out in Figure.6. Firstly, zero-mean Gaussian noise with standard deviation  $\delta = 0.01$  is added on the raw real-world underwater image. To capture most noise in detail layer  $d_1$ , the smoother parameter  $\lambda_1$  is adjusted to  $\lambda_1 = 0.25$  when producing  $u^1$ , which makes  $u^1$  more smoother than the input  $R$ . Secondly, to prevent noise from being boosted significantly, the enhancement coefficient  $\omega_1$  of  $d_1$  can be set to a sufficient small value (e.g.  $\omega_1 = 0.01$ ). Thus, visibility of the fuzzy input underwater image could be restored efficiently, and significant amplification of noise can be avoided. PSNR values of the input noisy underwater image and restoration results obtained by different parameter settings are illustrated in Figure.6.

As can be seen in Fig.7, noise is easily amplified by existing underwater restoration methods. While both subjective and objective results reveal that the proposed method

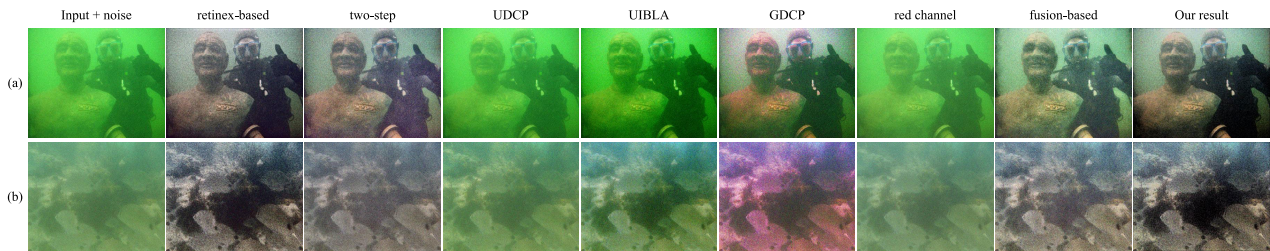


FIGURE 7. The performance of noise suppression among different methods.

TABLE 1. PSNR values of different methods in Figure.7.

Image	noisy raw	retinex-based	two-step	UDCP	UIBLA	GDCP	red channel	fusion based	Our result
(a)	11.6898	15.7913	12.4709	11.5966	10.2397	12.7955	12.4348	13.4863	<b>16.4929</b>
(b)	13.3390	13.4743	12.8923	13.0586	12.1945	10.9610	13.5735	12.0177	<b>15.8269</b>

can effectively improve the visibility of the raw underwater images without significant amplification of noise, as shown in Figure.7 and Table.1.

### B. QUALITATIVE EVALUATION

In Figure.8, the results of different methods and the corresponding reference images are shown. These test images are selected from the UIEB [11] and represent different underwater color tones and lighting conditions.

Due to the severe absorption of light, underwater images are usually captured in low-light conditions, as shown in Figure.8(a). It can be seen from the results, the retinex-based [5], two-step [17], fusion-based [3] and the proposed methods can generate visually pleasing results, while UIBLA [23], GDCP [36] and red channel [18] tend to produce unnatural appearance since the results are too bright for visual perception. UDCP [9] cannot handle the low-light circumstance properly. However, in the dark background region, the proposed method shows excellent performance in detail enhancement, even better than the reference image. Since light attenuation under water is wavelength-dependent, red light disappears firstly followed by green light and blue light, which results in greenish or bluish underwater images, as shown in Figure.8(b)(c)(d)(g). Due to the limitations of assumptions and priors, UDCP [9], GDCP [36] and UIBLA [23] aggravate the effect of color distortion. Two-step [17] and red channel [18] methods have less positive effect on the contrast enhancement, especially in Figure.8(c)(d). Haze still remains in the results. Fusion-based [3] method can effectively improve the contrast of underwater images but fails in color correction when dealing with the bluish image like Figure.8(g). The proposed method gains comparable results to the retinex-based [5] method, but is superior to it in terms of preserving details. What's more, as shown in Figure.8(e)(f), the proposed method can effectively remove the effect of haze and improve visibility.

In Figure.9, comparisons with above mentioned methods on restoring the challenging images in UIEB dataset

are presented. As can be seen, challenging underwater images have relatively low visibility and weak illumination. Under these conditions, all the physical-model based methods (e.g., UDCP [9], UIBLA [23], GDCP [36] and red channel [18]) fail to estimate transmission and veiling light accurately, which results in visually displeasing restoration results. For the scenes in Fig.9(c), both green seaweed and red fish exist in the bluish and low-light circumstance, two-step [17] and red channel [18] methods cannot handle this case properly. Although retinex-based [5] and fusion-based [3] methods can effectively remove color cast, improve contrast and brightness, unnatural artifacts in the high backscatter region (e.g., distant region in Figure.9(e)) and reddish color deviation (e.g., reddish rock in Figure.9(e)) are tend to be introduced.

To demonstrate the advantages achieved by the proposed method, we also compare it against several representative deep-learning based methods in Figure.10. As can be seen from the results produced by WaterGAN [27], obvious artifacts are introduced and the visibility of the restored images is severely unsatisfactory. In addition, UGAN [29] and UWCNN [28] have very little effect on color correction and contrast improvement, even increase the color cast. It is because that lacking sufficient training data will severely limit the performance of deep-learning based algorithms in the diverse water types and light conditions. By training the network using the real-world underwater dataset UIEB, the Water-Net [11] tends to produce visually pleasing results. However, it is noticeable that the proposed method achieves better visual quality than it with more natural appearance and better details.

In summary, the proposed method has a relatively decent performance for diverse water types and lighting conditions.

### C. QUANTITATIVE EVALUATION

Furthermore, in order to quantitatively evaluate the performance of the proposed method, both full-reference evaluation and non-reference evaluation are performed.



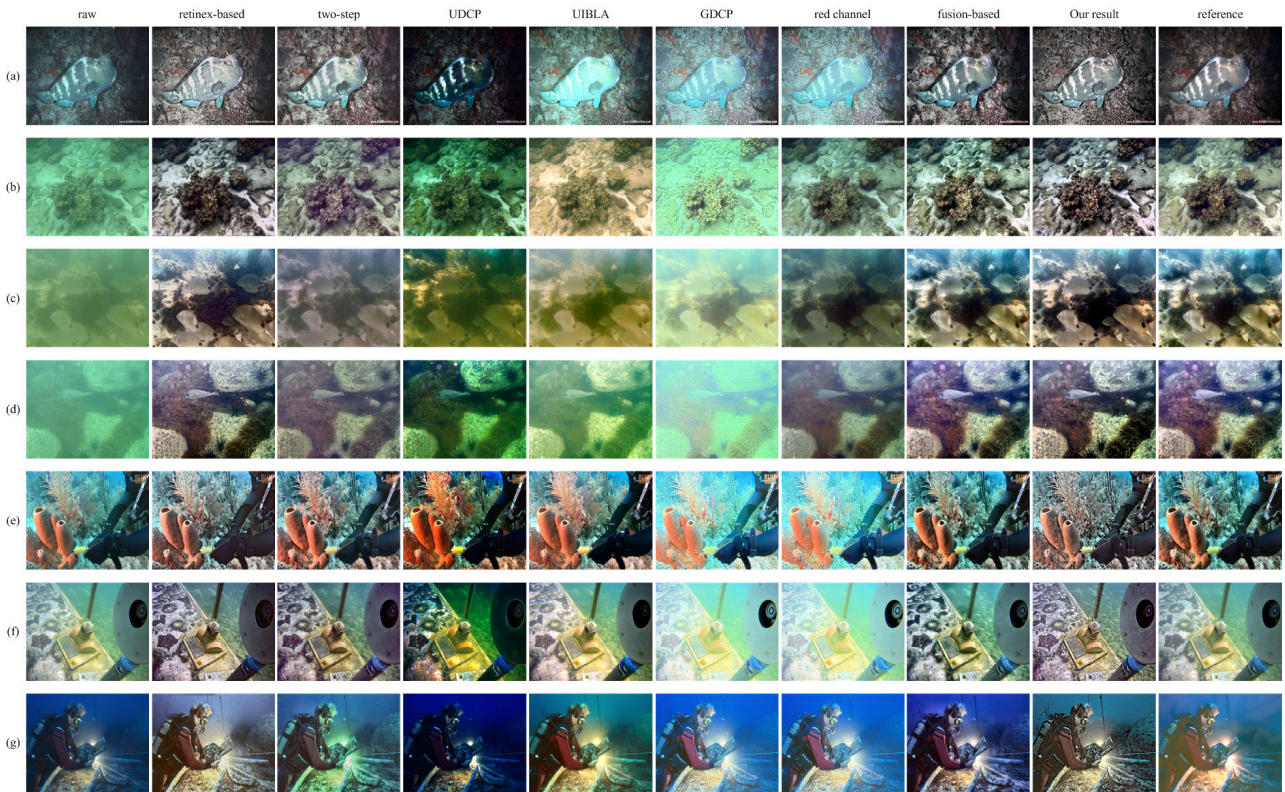


FIGURE 8. Subjective comparisons on underwater images from UIBE testing set.

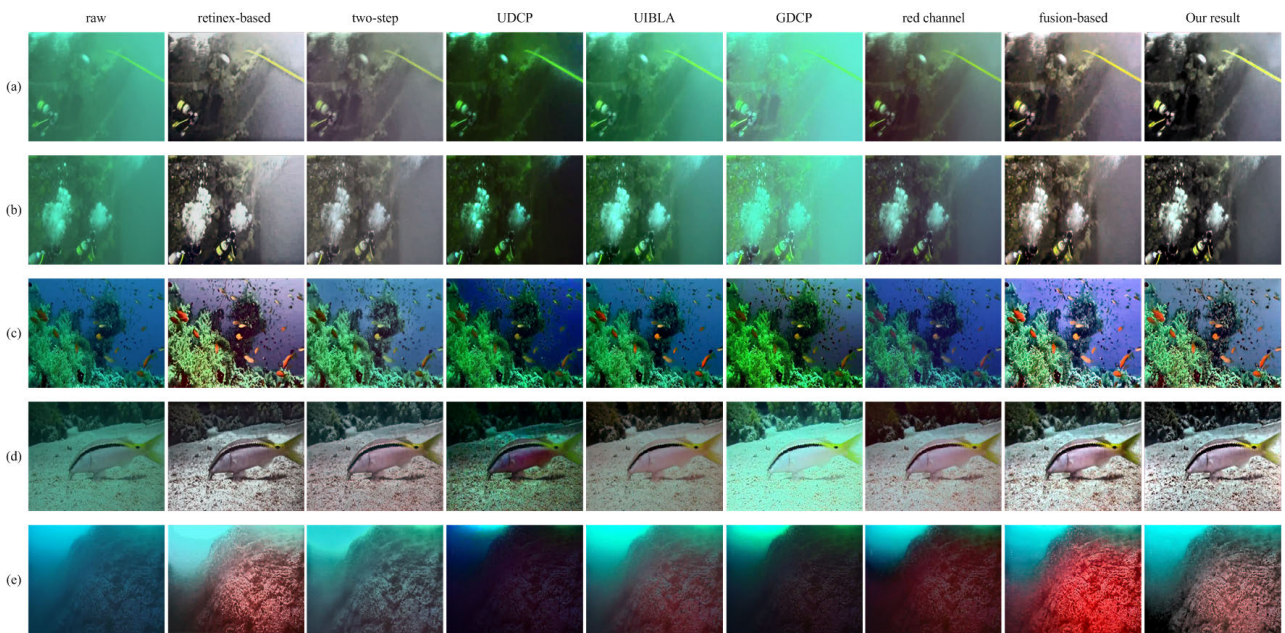


FIGURE 9. Subjective comparisons on underwater images from UIBE challenging set.

For full-reference evaluation, we treat the reference images supported by UIEB as the ground truths and compute the PSNR, PCQI between the restored results and the corresponding reference. A higher PSNR value means the result is closer

to the reference in terms of image content, while a higher PCQI score denotes better contrast variations for human perception. Table.2 represents the full-reference image quality evaluation of different methods on Figure.8.

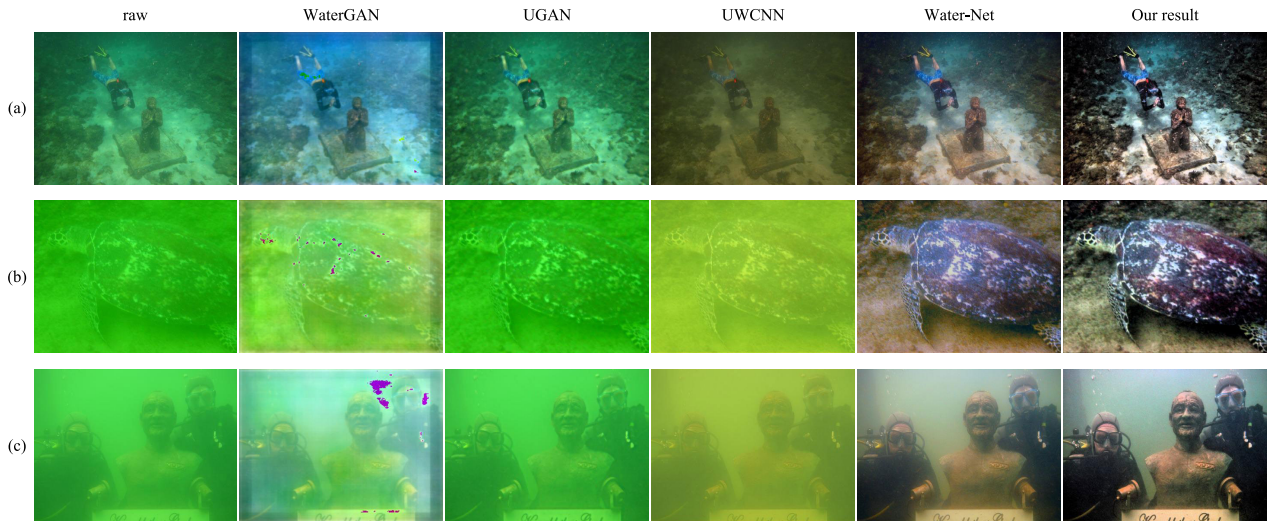


FIGURE 10. Subjective comparisons with deep-learning based methods.

TABLE 2. PSNR and PCQI values of different methods in Figure.8.

	retinex-based		two-step		UDCP		UIBLA		GDCP		red channel		fusion-based		Our result	
	PSNR	PCQI	PSNR	PCQI	PSNR	PCQI	PSNR	PCQI	PSNR	PCQI	PSNR	PCQI	PSNR	PCQI	PSNR	PCQI
(a)	16.5875	0.9605	15.2460	1.0397	15.4451	0.7953	12.3164	0.8676	10.1681	0.8917	22.5900	0.8224	18.8037	1.1381	<b>22.6353</b>	<b>1.1982</b>
(b)	19.9224	0.8654	19.6075	0.9638	13.5854	0.7436	17.6865	0.8051	11.4038	0.6765	<b>24.8341</b>	0.8569	21.1953	<b>1.1329</b>	21.1940	<b>1.1141</b>
(c)	19.9762	0.6477	16.9488	0.4498	12.2590	0.4304	16.8506	0.4176	10.5903	0.3895	14.4502	0.4034	<b>56.4846</b>	<b>0.9978</b>	<b>20.724</b>	<b>0.6631</b>
(d)	22.5723	0.7393	18.0688	0.6097	12.3602	0.5789	15.7605	0.4976	8.9734	0.3684	19.5161	0.4962	<b>67.3058</b>	<b>1.0000</b>	<b>22.7128</b>	<b>0.7812</b>
(e)	20.1712	0.7752	23.4547	0.9100	15.9820	0.7951	19.3308	0.7683	11.6426	0.6774	15.5774	0.6157	<b>74.4391</b>	<b>1.0000</b>	<b>27.7975</b>	<b>0.9264</b>
(f)	16.7914	0.9465	16.7732	1.0226	10.4533	0.8454	23.9415	1.0315	13.0704	0.8215	<b>24.4206</b>	0.9511	18.8038	<b>1.1104</b>	18.3155	<b>1.0880</b>
(g)	17.3542	0.9019	<b>19.0401</b>	<b>1.0878</b>	10.6714	0.6015	18.2677	1.0545	16.6730	1.0680	13.4663	0.7527	16.6886	1.0400	16.7624	0.9282

TABLE 3. UIQM and UCIQE values of different methods in Figure.8.

	retinex-based		two-step		UDCP		UIBLA		GDCP		red channel		fusion-based		Our result	
	UIQM	UCIQE	UIQM	UCIQE	UIQM	UCIQE	UIQM	UCIQE	UIQM	UCIQE	UIQM	UCIQE	UIQM	UCIQE	UIQM	UCIQE
(a)	1.2935	0.5276	1.3800	0.5322	<b>1.6125</b>	<b>0.5881</b>	1.2652	0.5734	1.2828	0.5479	1.1757	0.5702	1.5039	0.5821	1.5775	0.5784
(b)	1.5157	0.5579	1.5212	0.4958	1.5352	0.5467	1.3567	0.5152	1.3377	0.4362	1.4122	0.5315	<b>1.5891</b>	<b>0.5877</b>	1.5808	0.5807
(c)	1.1899	0.6008	0.8517	0.4458	1.0702	0.5499	0.8047	0.5267	0.7914	0.4585	0.9095	0.5289	1.3837	0.6474	<b>1.4195</b>	<b>0.6838</b>
(d)	1.3700	0.5729	1.1731	0.4584	1.4383	0.5935	1.0122	0.4783	0.9196	0.3741	1.0646	0.5088	1.4606	<b>0.6165</b>	<b>1.5374</b>	0.6152
(e)	1.1976	0.6013	1.2901	0.6410	1.4418	<b>0.7170</b>	1.2676	0.6834	1.1971	0.6470	0.9615	0.6039	1.3519	0.6538	<b>1.5213</b>	0.6880
(f)	1.1246	0.5886	1.1862	0.5934	1.3527	<b>0.6772</b>	1.0267	0.6368	0.9761	0.6039	0.8584	0.5777	1.1815	0.6145	<b>1.4618</b>	0.6668
(g)	1.2372	0.5993	1.4313	0.5889	1.7352	0.5908	1.4589	0.6817	1.3535	0.6045	1.4276	0.5894	1.5904	0.6445	<b>1.7519</b>	<b>0.6972</b>

As shown in Table.2, the fusion-based method [3] tends to have the relatively decent performance on both the PSNR and PCQI values. That is because most of reference images in UIEB are selected from the restoration results produced by the fusion-based technology. Beyond that, the proposed method ranks the second results. Although several values of two-step [3] and red channel [18] methods are higher than other methods, it can be seen from the corresponding subjective results that they are not consistent satisfactory.

Table.3, Table.4 and Table.5 quantitatively evaluate the performance of different methods on Figure.8, Figure.9

and Figure.10 in terms of non-reference criteria, e.g. UIQM and UCIQE. A higher UIQM value indicates a visually appealing result in human visual perception, while a higher UCIQE value means the result has better chroma, saturation and contrast.

In Table.3, the proposed method obtains almost the best scores of UIQM, while UCIQE values are comparable or slightly higher than fusion-based method [3]. We note that UDCP yields the best scores in Figure.8(a)(e)(f), but causes over-saturation or shortcoming in brightness adjustment actually.

TABLE 4. UIQM and UCIQE values of different methods in Figure.9.

	retinex-based		two-step		UDCP		UIBLA		GDPC		red channel		fusion-based		Our result	
	UIQM	UCIQE	UIQM	UCIQE	UIQM	UCIQE	UIQM	UCIQE	UIQM	UCIQE	UIQM	UCIQE	UIQM	UCIQE	UIQM	UCIQE
(a)	0.8702	0.5302	0.6634	0.4494	0.9562	0.5567	0.6272	0.5001	0.5218	0.4117	0.7202	0.5426	0.9323	0.5741	<b>1.1468</b>	<b>0.5761</b>
(b)	1.0486	0.5432	0.7811	0.4716	1.0739	0.5602	0.8563	0.5677	0.6648	0.4585	0.8026	0.5508	1.0511	0.5871	<b>1.2178</b>	<b>0.5879</b>
(c)	1.3377	0.5935	1.1634	0.5853	1.4746	0.5898	1.3809	0.6079	1.4442	0.6293	1.1606	0.5098	1.3800	0.6136	<b>1.5285</b>	<b>0.6427</b>
(d)	1.1443	0.5393	1.0920	0.5254	1.3147	0.5385	0.9234	0.4978	0.9537	0.5140	0.9358	0.5382	1.2126	<b>0.5878</b>	<b>1.3389</b>	0.5811
(e)	1.1545	0.6498	0.9346	0.5463	1.2396	0.5653	0.9483	0.6426	1.1226	0.6241	1.1409	0.6683	<b>1.4792</b>	<b>0.7239</b>	1.4734	0.6905

TABLE 5. UIQM and UCIQE values of different methods in Figure.10.

	WaterGAN		UGAN		UWCNN		Water-Net		Our result	
	UIQM	UCIQE	UIQM	UCIQE	UIQM	UCIQE	UIQM	UCIQE	UIQM	UCIQE
(a)	0.6066	0.4902	0.8300	0.4487	0.7468	0.4178	1.2030	0.5802	<b>1.4908</b>	<b>0.6251</b>
(b)	0.6766	0.3737	0.6831	0.3390	0.5306	0.3188	1.3408	0.5718	<b>1.3934</b>	<b>0.6015</b>
(c)	0.4642	0.4537	0.6320	0.3610	0.5617	0.3678	1.1223	0.5558	<b>1.3678</b>	<b>0.5933</b>

It's also worth mentioning that the proposed method stands out as the best performer across the two metrics in Table.4 as before. However, the phenomenon that the assessments are biased towards over-enhancement results still exists in other methods.

Consistent with the subjective performance, the proposed approach receives the highest scores of both UIQM and UCIQE comparing with deep-learning based methods in Table.5, which indicates that our method has more robust performance.

In summary, unless the gap between the current image quality evaluation criteria and the subjective visual quality, the proposed method shows excellent performance in improving the visibility of underwater images meanwhile suppressing the amplification of noise. Both qualitative and quantitative experiments demonstrate the effectiveness of the proposed method.

## V. CONCLUSION

In this paper, a multi-purpose oriented method is proposed to restore real-world underwater images. To compensate the attenuation of brightness, color and contrast, we try to capture different information into the corresponding layer in order to carry out the post-processing respectively. Firstly, a retinex model is used to separate the illumination which represents the variance of brightness from the reflectance. Then, the reflectance is decomposed into multiple scales. Color correction is implemented on the most smoothed base layer, while contrast enhancement is enforced on the gradient domain of the detail layers. In this way, the proposed method tends to generate visually pleasing results with improved brightness, contrast and color. In addition, the inevitable amplification of noise in conventional methods has also been overcome. Both qualitative and quantitative comparisons

indicate that the proposed method has superior robustness, accuracy and flexibility for diverse water types.

Nevertheless, the proposed method is not without limitations. The final result is easily affected by the estimation accuracy of the illumination and reflectance. What's more, over-enhancement still exhibits when dealing with pure white regions (such as the air bubbles in water). In the future work, we will focus on dealing with these issues.

## REFERENCES

- [1] C. Tan, G. Seet, A. Sluzek, and D. He, "A novel application of range-gated underwater laser imaging system (ULIS) in near-target turbid medium," *Opt. Lasers Eng.*, vol. 43, no. 9, pp. 995–1009, Sep. 2005.
- [2] Y. Y. Schechner and Y. Averbuch, "Regularized image recovery in scattering media," *IEEE Trans. Pattern Anal. Mach. Intell.*, vol. 29, no. 9, pp. 1655–1660, Sep. 2007.
- [3] C. Ancuti, C. O. Ancuti, T. Haber, and P. Bekaert, "Enhancing underwater images and videos by fusion," in *Proc. IEEE Conf. Comput. Vis. Pattern Recognit.*, Jun. 2012, pp. 81–88.
- [4] S. Zhang, T. Wang, J. Dong, and H. Yu, "Underwater image enhancement via extended multi-scale Retinex," *Neurocomputing*, vol. 245, pp. 1–9, Jul. 2017.
- [5] X. Fu, P. Zhuang, Y. Huang, Y. Liao, X.-P. Zhang, and X. Ding, "A retinex-based enhancing approach for single underwater image," in *Proc. IEEE Int. Conf. Image Process. (ICIP)*, Oct. 2014, pp. 4572–4576.
- [6] C. Dai, M. Lin, J. Wang, and X. Hu, "Dual-purpose method for underwater and low-light image enhancement via image layer separation," *IEEE Access*, vol. 7, pp. 178685–178698, 2019.
- [7] K. He, J. Sun, and X. Tang, "Single image haze removal using dark channel prior," *IEEE Trans. Pattern Anal. Mach. Intell.*, vol. 33, no. 12, pp. 2341–2353, Dec. 2011.
- [8] J. Y. Chiang and Y.-C. Chen, "Underwater image enhancement by wavelength compensation and dehazing," *IEEE Trans. Image Process.*, vol. 21, no. 4, pp. 1756–1769, Apr. 2012.
- [9] P. L. J. Drews, E. R. Nascimento, S. S. C. Botelho, and M. F. M. Campos, "Underwater depth estimation and image restoration based on single images," *IEEE Comput. Graph. Appl.*, vol. 36, no. 2, pp. 24–35, Mar. 2016.
- [10] S. Yang, Z. Chen, Z. Feng, and X. Ma, "Underwater image enhancement using scene depth-based adaptive background light estimation and dark channel prior algorithms," *IEEE Access*, vol. 7, pp. 165318–165327, 2019.

- [11] C. Li, C. Guo, W. Ren, R. Cong, J. Hou, S. Kwong, and D. Tao, "An underwater image enhancement benchmark dataset and beyond," *IEEE Trans. Image Process.*, vol. 29, pp. 4376–4389, 2020.
- [12] X. Ding, Y. Wang, Y. Yan, Z. Liang, Z. Mi, and X. Fu, "Jointly adversarial network to wavelength compensation and dehazing of underwater images," 2019, *arXiv:1907.05595*. [Online]. Available: <http://arxiv.org/abs/1907.05595>
- [13] B. L. McGlamery, "A computer model for underwater camera systems," *Proc. SPIE*, vol. 208, pp. 221–231, Mar. 1980.
- [14] Y. Wang, W. Song, G. Fortino, L.-Z. Qi, W. Zhang, and A. Liotta, "An experimental-based review of image enhancement and image restoration methods for underwater imaging," *IEEE Access*, vol. 7, pp. 140233–140251, 2019.
- [15] C. O. Ancuti, C. Ancuti, C. De Vleeschouwer, and M. Sbert, "Color channel compensation (3C): A fundamental pre-processing step for image enhancement," *IEEE Trans. Image Process.*, vol. 29, pp. 2653–2665, 2020.
- [16] K. Iqbal, M. Odetayo, A. James, R. A. Salam, and A. Z. H. Talib, "Enhancing the low quality images using unsupervised colour correction method," in *Proc. IEEE Int. Conf. Syst., Man Cybern.*, Oct. 2010, pp. 1703–1709.
- [17] X. Fu, Z. Fan, M. Ling, Y. Huang, and X. Ding, "Two-step approach for single underwater image enhancement," in *Proc. Int. Symp. Intell. Signal Process. Commun. Syst. (ISPACS)*, Nov. 2017, pp. 789–794.
- [18] A. Galdran, D. Pardo, A. Picón, and A. Alvarez-Gila, "Automatic red-channel underwater image restoration," *J. Vis. Commun. Image Represent.*, vol. 26, pp. 132–145, Jan. 2015.
- [19] H. Wen, Y. Tian, T. Huang, and W. Gao, "Single underwater image enhancement with a new optical model," in *Proc. IEEE Int. Symp. Circuits Syst. (ISCAS)*, May 2013, pp. 753–756.
- [20] P. Drews, Jr., E. do Nascimento, F. Moraes, S. Botelho, and M. Campos, "Transmission estimation in underwater single images," in *Proc. IEEE Int. Conf. Comput. Vis. Workshops*, Dec. 2013, pp. 825–830.
- [21] S. Emberton, L. Chittka, and A. Cavallaro, "Hierarchical rank-based veiling light estimation for underwater dehazing," in *Proc. Brit. Mach. Vis. Conf.*, 2015, pp. 125.1–125.12.
- [22] N. Carlevaris-Bianco, A. Mohan, and R. M. Eustice, "Initial results in underwater single image dehazing," in *Proc. OCEANS MTS/IEEE SEAT-TLE*, Sep. 2010, pp. 1–8.
- [23] Y.-T. Peng and P. C. Cosman, "Underwater image restoration based on image blurriness and light absorption," *IEEE Trans. Image Process.*, vol. 26, no. 4, pp. 1579–1594, Apr. 2017.
- [24] Y. Li, J. Li, Y. Li, H. Kim, and S. Serikawa, "Low-light underwater image enhancement for deep-sea tripod," *IEEE Access*, vol. 7, pp. 44080–44086, 2019.
- [25] H.-H. Chang, "Single underwater image restoration based on adaptive transmission fusion," *IEEE Access*, vol. 8, pp. 38650–38662, 2020.
- [26] S. Mandal and A. N. Rajagopalan, "Local proximity for enhanced visibility in haze," *IEEE Trans. Image Process.*, vol. 29, pp. 2478–2491, 2020.
- [27] J. Li, K. A. Skinner, R. M. Eustice, and M. Johnson-Roberson, "WaterGAN: Unsupervised generative network to enable real-time color correction of monocular underwater images," *IEEE Robot. Autom. Lett.*, vol. 3, no. 1, pp. 387–394, Jan. 2018.
- [28] C. Li, S. Anwar, and F. Porikli, "Underwater scene prior inspired deep underwater image and video enhancement," *Pattern Recognit.*, vol. 98, pp. 107038–107049, Feb. 2020.
- [29] C. Fabbri, M. J. Islam, and J. Sattar, "Enhancing underwater imagery using generative adversarial networks," in *Proc. IEEE Int. Conf. Robot. Autom. (ICRA)*, May 2018, pp. 7159–7165.
- [30] C. Li, J. Guo, and C. Guo, "Emerging from water: Underwater image color correction based on weakly supervised color transfer," *IEEE Signal Process. Lett.*, vol. 25, no. 3, pp. 323–327, Mar. 2018.
- [31] Y. Guo, H. Li, and P. Zhuang, "Underwater image enhancement using a multiscale dense generative adversarial network," *IEEE J. Ocean. Eng.*, early access, Jun. 4, 2019, doi: [10.1109/JOE.2019.2911447](https://doi.org/10.1109/JOE.2019.2911447).
- [32] X. Fu, D. Zeng, Y. Huang, X.-P. Zhang, and X. Ding, "A weighted variational model for simultaneous reflectance and illumination estimation," in *Proc. IEEE Conf. Comput. Vis. Pattern Recognit. (CVPR)*, Jun. 2016, pp. 2782–2790.
- [33] T. Goldstein and S. Osher, "The split bregman method for L1-regularized problems," *SIAM J. Imag. Sci.*, vol. 2, no. 2, pp. 323–343, Jan. 2009.
- [34] Z. Farbman, R. Fattal, D. Lischinski, and R. Szeliski, "Edge-preserving decompositions for multi-scale tone and detail manipulation," *ACM Trans. Graph.*, vol. 27, no. 3, pp. 67–76, 2008.
- [35] J.-P. Tarel and N. Hautiere, "Fast visibility restoration from a single color or gray level image," in *Proc. IEEE 12th Int. Conf. Comput. Vis.*, Kyoto, Japan, Sep. 2009, pp. 2201–2208.
- [36] Y.-T. Peng, K. Cao, and P. C. Cosman, "Generalization of the dark channel prior for single image restoration," *IEEE Trans. Image Process.*, vol. 27, no. 6, pp. 2856–2868, Jun. 2018.
- [37] S. Wang, K. Ma, H. Yeganeh, Z. Wang, and W. Lin, "A patch-structure representation method for quality assessment of contrast changed images," *IEEE Signal Process. Lett.*, vol. 22, no. 12, pp. 2387–2390, Dec. 2015.
- [38] K. Panetta, C. Gao, and S. Agaian, "Human-visual-system-inspired underwater image quality measures," *IEEE J. Ocean. Eng.*, vol. 41, no. 3, pp. 541–551, Jul. 2016.
- [39] M. Yang and A. Sowmya, "An underwater color image quality evaluation metric," *IEEE Trans. Image Process.*, vol. 24, no. 12, pp. 6062–6071, Dec. 2015.



**ZETIAN MI** received the B.S. and Ph.D. degrees from the College of Computer Science and Technology, Sichuan University, Chengdu, China, in 2012 and 2017, respectively. She is currently a Lecturer with the College of Information Science and Technology, Dalian Maritime University. Her main research interests include image processing and machine learning.



**YUANYUAN LI** received the B.S. degree in computer science and technology from Qufu Normal University, Qufu, China, in 2019. She is currently pursuing the M.S. degree with Dalian Maritime University. Her research interests include computer vision and low-light image enhancement.



**YAFEI WANG** received the Ph.D. degree in electronics science and technology from the Dalian University of Technology, Dalian, China, in 2018. He is currently a Postdoctoral Research Fellow with Dalian Maritime University. His research interests include image processing, computer vision, eye gaze tracking, and machine learning.



**XIANPING FU** received the Ph.D. degree in communication and information system from Dalian Maritime University, Dalian, China, in 2005. From 2008 to 2009, he was a Postdoctoral Fellow with the Harvard Medical School, Schepens Eye Research Institute, Boston, MA, USA. He is currently a Professor with the Information Science and Technology College, Dalian Maritime University. His research interests include perception of natural scenes in engineering systems, including multimedia, image/video processing, and object recognition.

...